Identification and Functional Characterization of Protein Kinase A-catalyzed Phosphorylation of Potassium Channel Kv1.2 at Serine 449*

Rosalyn P. Johnson[‡1], Ahmed F. El-Yazbi[‡], Morgan F. Hughes[§], David C. Schriemer[§], Emma J. Walsh[‡], Michael P. Walsh[‡2], and William C. Cole[‡3]

From the [‡]Smooth Muscle Research Group and [§]Southern Alberta Mass Spectrometry Centre, University of Calgary, Calgary, Alberta T2N 4N1, Canada

Vascular smooth muscle Kv1 delayed rectifier K^+ channels (K_{DR}) containing Kv1.2 control membrane potential and thereby regulate contractility. Vasodilatory agonists acting via protein kinase A (PKA) enhance vascule smooth muscle Kv1 activity, but the molecular basis of this regulation is uncertain. We characterized the role of a C-terminal phosphorylation site, Ser-449, in Kv1.2 expressed in HEK 293 cells by biochemical and electrophysiological methods. We found that 1) *in vitro* phosphorylation of Kv1.2 occurred exclusively at serine residues, 2) one major phosphopeptide that co-migrated with [449]pSASTISK was generated by proteolysis of *in vitro* phosphorylated Kv1.2, 3) the peptide [445]KKSRSASTISK exhibited stoichiometric phosphorylation by PKA *in vitro*, 4) matrix-assisted laser desorption ionization time-of-flight (MALDI-TOF) mass spectroscopy (MS) and MS/MS confirmed *in vitro* Ser-449 phosphorylation by PKA, 5) *in situ* phosphorylation at Ser-449 was detected in HEK 293 cells by MALDI-TOF MS followed by MS/MS. MIDAS (multiple reaction monitoring-initiated detection and sequencing) analysis revealed additional phosphorylated residues, Ser-440 and Ser-441, 6) *in vitro* ^{32}P incorporation was significantly reduced in Kv1.2-S449A, Kv1.2-S449D, and Kv1.2-S440A/S441A/S449A mutant channels, but Kv1.2-S440A/S441A was identical to wild-type Kv1.2 (Kv1.2-WT), and 7) bath applied 8-Br-cAMP or dialysis with PKA catalytic subunit (cPKA) increased Kv1.2-WT but not Kv1.2-S449A current amplitude. cPKA increased Kv1.2-WT current in inside-out patches. Rp-CPT-cAMPS reduced Kv1.2-WT current, blocked the increase due to 8-Br-cAMP, but had no effect on Kv1.2-S449A. cPKA increased current due to double mutant Kv1.2-S440A/S441A but had no effect on Kv1.2-S449D or Kv1.2-S440A/S441A/S449A. We conclude that Ser-449 in Kv1.2 is a site of PKA phosphorylation and a potential molecular mechanism for Kv1-containing K_{DR} channel modulation by agonists via PKA activation.

Voltage-gated K^+ channels (Kv)[4] composed of members of the Kv1 family (Kv1) are expressed in vascular smooth muscle (VSM) and other excitable cells, where they play an important role in controlling membrane potential, a key mechanism for regulation of contraction and arterial diameter (1). Steady-state Ca^{2+} influx through voltage-gated Ca^{2+} channels, resulting in elevated cytosolic Ca^{2+} concentration and contraction, requires sustained depolarization. In contrast, Kv1 channel activation induces hyperpolarization, reduces voltage-gated Ca^{2+} channel open probability, and promotes relaxation (1–3).

Phosphorylation of ion channels by protein kinases is an important mechanism by which ion channel gating (opening and closing) and, thereby, membrane potential are modulated by cellular signaling pathways. VSM Kv1 channels containing Kv1.2-Kv1.5 (4–6) alone or with Kv1.6 (7) contribute to control of arterial diameter by vasoconstrictor and vasodilator stimuli (8–13). For example, hyperpolarization and relaxation induced by elevations in intracellular (cAMP) are suppressed by the block of Kv1 channels (14–18), and the activity of Kv1-containing VSM K_{DR} is enhanced by protein kinase A (PKA) (10–13, 19–22). However, the molecular basis of this regulation is unclear.

Previous studies showed that gating of Kv1.2 channels expressed in *Xenopus* oocytes is stimulated by PKA (23), similar to VSM K_{DR} channels, which contain this pore-forming Kv1 subunit (7–13). There are six potential PKA phosphorylation sites within the cytoplasmic regions of Kv1.2 (see Fig. 1, *A* and *B*) based on the consensus motif Arg/Lys-Xaa-Xaa-Ser/Thr (24). An N-terminal residue, Thr-46, was proposed to be the site of PKA phosphorylation, as mutation to valine (T46V) prevented modulation by β-adrenoreceptor activation or exposure to the catalytic subunit of PKA (cPKA) (23). However, this conclusion has been questioned based on structural analysis of the N-terminal domain and the positive shift in voltage-dependent gating produced by the T46V mutation (25). Sites Ser-440, Ser-441, and Ser-449 near the C terminus were recently identified

[4] The abbreviations used are: Kv, voltage-gated potassium channel; VSM, vascular smooth muscle; K_{DR}, delayed rectifier potassium channel; PKA, protein kinase A; cPKA, catalytic subunit of PKA; MIDAS, multiple reaction monitoring-initiated detection and sequencing; MALDI-TOF, matrix-assisted laser desorption ionization time-of-flight; I-V, current-voltage; HEK, human embryonic kidney; MS, mass spectroscopy; pF, picofarads; WT, wild type; LC, liquid chromatography.

to be phosphorylated in Kv1.2 immunoprecipitates derived from brain as well as transfected human embryonic kidney (HEK 293) and COS-1 cells using a proteomic approach (26). Phosphorylation of these residues was suggested to be important for trafficking to the cell membrane (26), but the kinase(s) involved was not identified. cAMP/PKA-dependent signaling was reported to alter surface expression of Kv1.2, but phosphorylation at Ser-440 and Ser-449 was not required (27).

In the present study we used a combination of biochemical, mutagenesis, and electrophysiological analyses to 1) determine whether Kv1.2 is a substrate for PKA, 2) identify the PKA phosphorylation site(s) involved, and 3) determine whether phosphorylation of the identified residue(s) mediates PKA-dependent changes in Kv1.2 current amplitude.

EXPERIMENTAL PROCEDURES

Site-directed Mutagenesis and Myc-epitope Tagging—Kv1.2-T46A, -T46D, -S449A, -S449D, -S440A/S441A, and -S440A/S441A/S449A mutants were engineered from rabbit Kv1.2 (GenBank[TM] accession number AF284420) (see Fig. 1*B*) and subcloned into pcDNA3.1 by overlap extension using the PCR (12). Primer sequences were as follows (F and R are forward and reverse primers). 1) T46A: T7-F, 5′-GCTAGTTATTGCTCA-GCGG-3′; T46A-R, 5′-GGCCAAGGTCTTGAGCTGTGCC-TCAAACCGCAGCCCTGA-3′; T46A-F, 5′-TCAGGGCTGC-GGTTTGAGGCACAGCTCAAGACCTTGGCC-3′; ageI-R, 5′-AAGTACTGGGCCTGTTCCTCTC-3′. 2) T46D: T7-F, T46D-R 5′-GGCCAAGGTCTTGAGCTGATCCTCAAACC-GCAGCCCTGA-3′; T46D-F, 5′-TCAGGGCTGCGGTTTG-AGGATCAGCTCAAGACCTTGGCC-3′, ageI-R. 3) S449A: ageI-F, sp6-R, 5′-ATTTAGGTGACACTATAG-3′; S449A-R, 5′-AATGGTGGAGGCAACTCTACTTTTCTT-3′; S449A-F, 5′-AAGAAAAGTAGAGTTGCCTCCACCATT-3′. 4) S449D: ageI-F, sp6-R, S449D-R, 5′-AATGGTGGAGGCGTCTCTAC-TTTCTT-3′; S449A-F, 5′-AAGAAAAGTAGAGACGCCTC-CACCATT-3′. 5) S440A: ageI-F, sp6-R, S440A-F, 5′-GATCC-CAGCCTCCCCTG-3′; S440A-R, 5′-CAGGGGAGGCTGGG-ATC-3′. 6) S441A: ageI-F, sp6-R, S441A-F, 5′-CCCATCCGC-CCCTGACC-3′; S441A-R, 5′-GGTCAGGGGCGGATGGG-3′. 7) S440A/S441A: ageI-F, sp6-R, S440A/S441A-F, 5′-GATC-CCAGCCGCCCCTG-3′; S440A/S441A-R; 5′-CAGGGGCG-GCTGGGATC-3′. 8) S440A/S441A/S449A: S449A, primers for S440A and S441A.

A 10 residue c-Myc tag was added to the C terminus of each construct, and cDNAs from positive colonies were sequenced. Myc-tagged protein expressed in HEK 293 cells was recognized by anti-Kv1.2 and immunoprecipitated with anti-Myc (see Fig. 1, *C* and *D*).

Cell Culture and cDNA Transfection—HEK 293 cells were maintained and transfected as previously described (4, 5). For patch clamp experiments, cells were co-transfected with cDNAs encoding green fluorescent protein and channel constructs and studied within 48 h. For biochemical experiments, cells were grown to ~80% confluence, transfected with Kv1.2 constructs alone, and harvested after ~48 h.

Cell Lysate Preparation and Immunoprecipitation—HEK 293 cells were harvested, lysates were prepared, and Kv1.2-WT and mutant construct proteins were immunoprecipitated using Protein A-Sepharose beads (GE Healthcare), as previously described (5).

In Vitro Phosphorylation of Kv1.2-myc Proteins—Proteins were phosphorylated in 100 μl of buffer containing 20 mM Tris-HCl (pH 7.4), 1 mM EGTA, 5 mM MgCl$_2$, 5 mM NaF, 1 μM okadaic acid, and cPKA (0.1 μg/ml except for mass spectrometry at 1.0 μg/ml). Reactions were initiated with 0.2 mM ATP and 1.0 μCi/nmol [γ-^{32}P]ATP and terminated with Laemmli SDS buffer before elution from beads and separation by SDS-PAGE.

Immunoblotting—^{32}P-Labeled proteins on SDS-PAGE gels were transferred to nitrocellulose and immunoblotted as previously described (28) before exposure to Kodak XB-1 blue film and densitometric analysis using Image Master 1D software. Mean values $\pm$ S.E. were compared by unpaired Student's *t* test or analysis of variance followed by the Bonferroni post-hoc test; $p < 0.05$ was considered statistically significant.

Tryptic Digestion and Two-dimensional Peptide Mapping—L-1-Tosylamido-2-phenylethyl chloromethyl ketone-trypsin digestion of ^{32}P-labeled channel protein and phosphopeptide mapping were performed as previously described (29). Migration of ^{32}P-labeled tryptic peptides was compared with synthetic pSASTISK and detected by autoradiography and 0.25% ninhydrin in acetone.

Acid Hydrolysis and Phosphoamino Acid Analysis—Lyophilized tryptic peptides were resuspended in 6 M HCl (250 μl) for 2 h at 110 °C before drying, resuspension, mixing with phosphoserine, phosphothreonine, and phosphotyrosine standards and separation as previously described (30, 31). ^{32}P-Labeled residues and standards were detected by autoradiography and ninhydrin, respectively.

Immobilized Metal (Fe^{3+}) Affinity Chromatography—Immobilized metal (Fe^{3+}) affinity chromatography was performed using a 1-ml (0.7 $\times$ 2.5 cm) pre-packed HiTrap[TM] Chelating HP column (Amersham Biosciences) (32) charged with 50 mM ferric chloride. Lyophilized ^{32}P-labeled tryptic peptides were applied and eluted using a stepwise gradient from pH 6.0 to 9.5 in 0.5 increments, and radioactive content was assessed by Čerenkov counting.

Mass Spectrometric Analysis—Phosphorylated Kv1.2-Myc digests were acidified with trifluoroacetic acid and loaded on a self-packed cartridge (150 μm $\times$ 25 mm C18; Zorbax Stablebond C18, 300 Å, 5 μm), and the flow-through was analyzed by MALDI-TOF (Voyager DE-STR, Applied Biosystems, Foster City, CA). A fraction of the flow-through was analyzed by direct infusion nanospray MS/MS on an ion trap mass spectrometer (XCT Ultra, Agilent Technologies) to determine the fragmentation pattern of the *m/z* 773.4 phosphorylated tryptic peptide detected using this method. The sequence was determined by 1) peptide fragment fingerprinting against Kv1.2 tryptic peptide sequences using the MASCOT search engine (Matrix Science, London, England), allowing for variable phosphorylation of Ser/Thr residues, and 2) manual sequencing. This approach was also used to identify Ser-449 phosphorylation *in situ* in control and 8-Br-cAMP-treated HEK 293 cells. A MIDAS (multiple reaction monitoring-initiated detection and sequencing) approach was also used to identify sites on Kv1.2 *in situ*. Tryptic
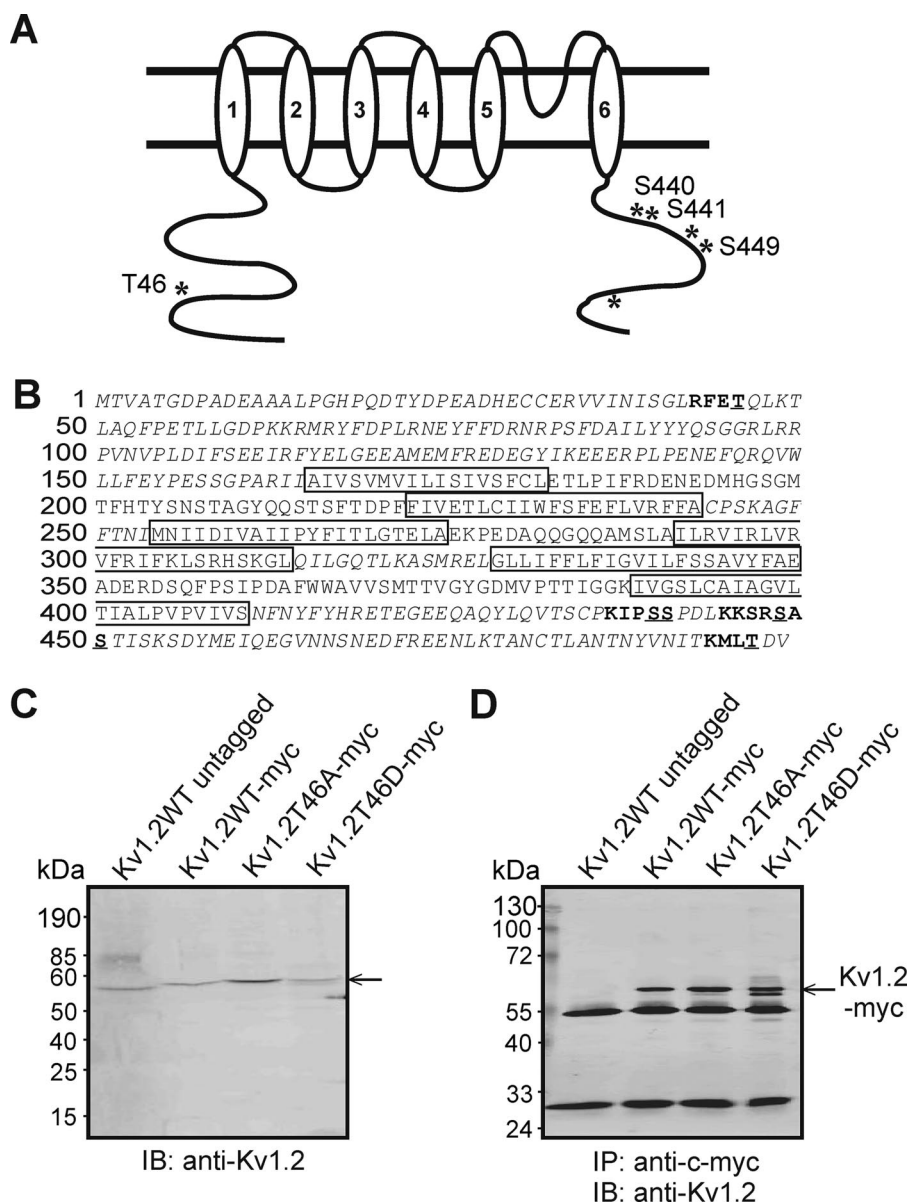
FIGURE 1. **Identification of potential PKA consensus phosphorylation sites in Kv1.2 and immunoprecipitation of Myc-tagged wild-type and mutant Kv1.2.** *A*, schematic of Kv1.2 with candidate PKA phosphorylation sites indicated by *asterisks*, and Ser/Thr residues relevant to the study are labeled. *B*, amino acid sequence of Kv1.2 indicating transmembrane domains (*boxes*), cytoplasmic domains (*italics*) assessed by MIDAS for phosphorylated residues, candidate PKA consensus sites (*bold*), and potential phosphorylated Ser/Thr residues (*underlined*). *C*, immunoblot (*IB*) analysis of untagged Kv1.2-WT and Myc-tagged WT and mutant constructs using anti-Kv1.2. *D*, immunoblot identification of untagged Kv1.2-WT and Myc-tagged WT and mutant constructs by anti-Kv1.2 in anti-Myc immunoprecipitates (*IP*).

Phosphorylation of Synthetic Peptides with cPKA—Synthetic peptides (KKSRSASTISK, KKSRAASTISK, and LLRRASLG) were used as substrate in phosphorylation reactions with cPKA and $[\gamma\text{-}^{32}\text{P}]$ATP as previously described (29). K_m and V_{max} values were calculated by linear regression analysis of Lineweaver-Burk and Eadie-Hofstee plots or by Michaelis-Menten analysis using KaleidaGraph software (Synergy Software, Reading, PA) and expressed as the mean ± S.E. of five experiments in triplicate. Peptide phosphorylation stoichiometry was determined as above, except cPKA was varied between 1.0 and 5.0 μg/ml, and peptide was fixed at 50 μM. Values are the means ± S.E. of three experiments in triplicate.

Patch Clamp Electrophysiology—Whole-cell currents due to Kv1.2-WT and mutant channel constructs in HEK 293 cells were recorded and analyzed as previously described (4, 12). Current-voltage (I-V) relations were determined using 250-ms step pulses between −80 and +30 mV or 5-s ramp pulses between −80 and +40 mV. Because of marked cell-to-cell variability in expressed channel protein density, current amplitudes were normalized to the value at +30 mV (step protocol) in control conditions for each cell for determination of the mean change in I-V relation due to PKA activation or inhibition. Current density (pA/pF) was determined by normalization to cell capacitance. Mean changes in I-V relation, current density, and fractional changes in current amplitude at +20 (steps) or +40 mV (ramps) were compared by unpaired Student's *t* test or analysis of variance followed by the Bonferroni post-hoc test.

Peptide Synthesis—Peptides were synthesized in the University of Calgary Peptide Synthesis Core Facility and purified as previously described (33). Amino acid sequence was confirmed by amino acid analysis and shown to be >95% pure by analytical high performance liquid chromatography.

Chemicals—$[\gamma\text{-}^{32}\text{P}]$ATP was purchased from ICN Biomedical Inc. cPKA was purified to electrophoretic homogeneity from bovine heart according to Demaille *et al.* (34). Protein A-Sepharose beads were obtained from GE Healthcare. All other chemicals were purchased from VWR or Sigma-Aldrich.

digests of HEK 293 Kv1.2 immunoprecipitates were reduced to dryness *in vacuo* and reconstituted in mobile phase A (0.1% formic acid, 3% acetonitrile in water). Sample was injected into a Dionex Ultimate 3000 nano-LC system configured with trap and separation columns (PepMap C18 reversed phase). Phosphorylation events were detected by MIDAS using a Qtrap 4000 MS (AB/MDS Analytical Technologies). All tryptic peptides derived from cytosolic regions of Kv1.2 (Fig. 1) were considered in this analysis to ensure high sensitivity while achieving a comprehensive survey of all potential intracellular phosphorylation sites on the channel protein.
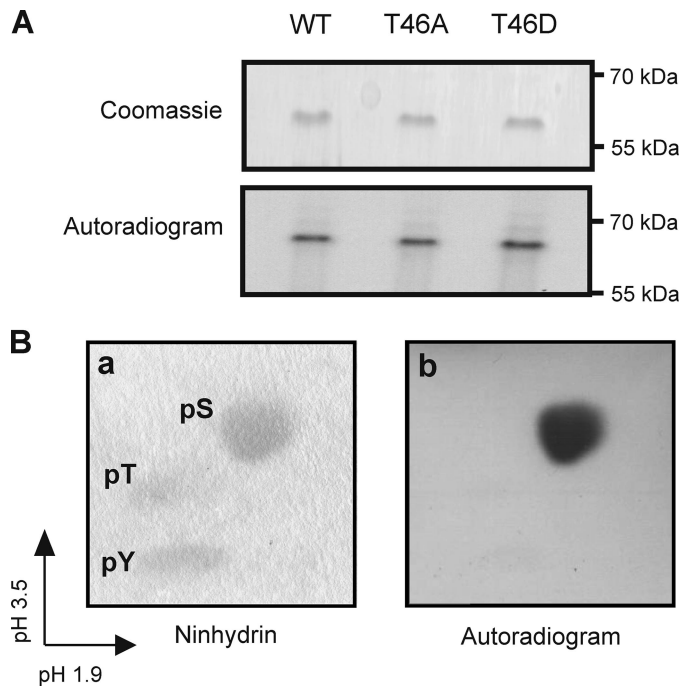
A

FIGURE 2. *In vitro* phosphorylation of Kv1.2 serine residue(s) by PKA. *A*, Kv1.2-WT-myc, -T46A-myc, and -T46D-myc immunoprecipitates treated with cPKA in the presence of [γ-^{32}P]ATP and visualized by Coomassie Blue staining and autoradiography to detect ^{32}P incorporation. Data are representative of six experiments. *B*, phosphoamino acid analysis of phosphorylated Kv1.2-WT-myc protein by two-dimensional electrophoresis. Unlabeled phosphoserine (*pS*), phosphothreonine (*pT*), and phosphotyrosine (*pY*) standards were detected by ninhydrin staining (*a*) and ^{32}P-labeled residues by autoradiography (*b*). Data are representative of four experiments.

RESULTS

T46A Does Not Abolish in Vitro Phosphorylation of Kv1.2 by PKA—To address the relevance of Thr-46, Myc-tagged Kv1.2-WT, Kv1.2-T46A, and Kv1.2-T46D proteins were immunoprecipitated from HEK 293 cell lysates with anti-Myc and phosphorylated *in vitro* with cPKA in the presence of [γ-^{32}P]ATP. Fig. 2*A* shows that Kv1.2-WT protein was phosphorylated by PKA, as were T46A and T46D mutant proteins. ^{32}P incorporation was not detected for reactions performed in the absence of cPKA (data not shown). This demonstrates that Kv1.2 is a substrate for PKA and sites other than Thr-46 are involved.

Kv1.2 Is Phosphorylated in Vitro Exclusively at Serine, Producing One Major Tryptic Phosphopeptide—To determine the identity of the amino acid residue(s) phosphorylated by PKA, tryptic digests of ^{32}P-labeled Kv1.2-WT were subjected to acid hydrolysis, mixed with phosphoserine, phosphothreonine, and phosphotyrosine, subjected to two-dimensional electrophoresis, and viewed by autoradiography. Fig. 2*B* shows that the phosphorylated residue(s) co-migrated with phosphoserine, detected by ninhydrin staining. Thus, Kv1.2 is phosphorylated by PKA *in vitro* exclusively at serine residues.

Phosphopeptide maps of Kv1.2-WT and T46A mutant are compared in Fig. 3*A*. A single major phosphopeptide of identical mobility was generated after digestion of both proteins. Minor spots in Fig. 3*A* represent <5% of the total radioactivity. This indicates that Kv1.2 is phosphorylated by PKA *in vitro* on one tryptic fragment. The presence of one major phosphorylated peptide was also indicated by separation of Kv1.2-WT

A

B

C
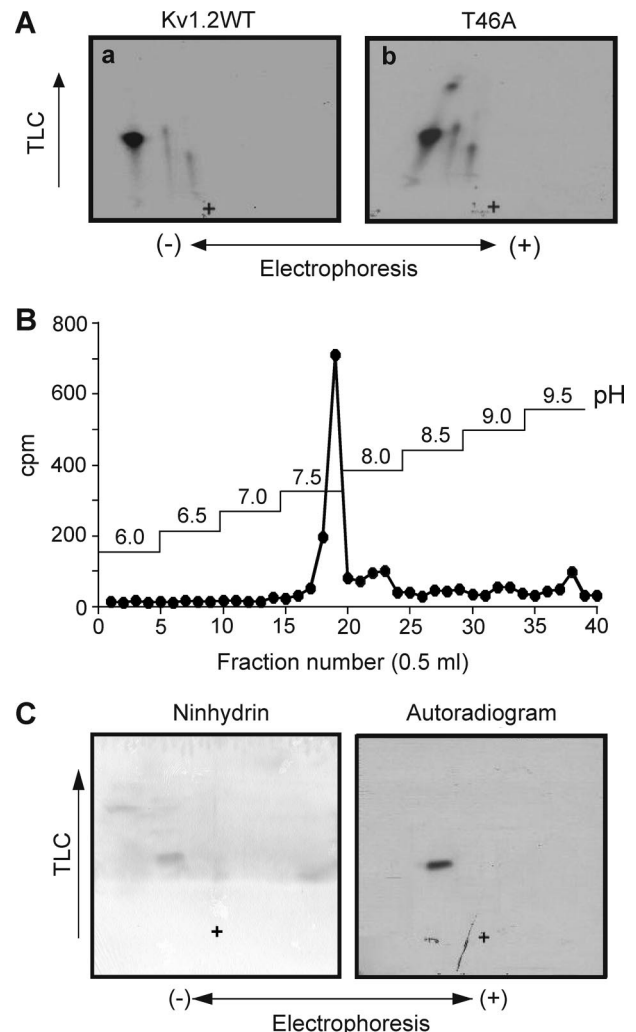
FIGURE 3. Phosphopeptide mapping and affinity purification of Kv1.2-WT and T46A phosphopeptides and pSASTISK co-migrates with tryptic phosphopeptide derived from PKA-phosphorylated Kv1.2-WT. *A*, phosphopeptide maps of Kv1.2-WT-myc (*a*) and -T46A-myc (*b*) phosphorylated by cPKA in the presence of [γ-^{32}P]ATP. Data are representative of six independent experiments. + indicates the origin. *B*, radioactivity profile of PKA-phosphorylated Kv1.2-WT-myc tryptic peptides separated by immobilized metal affinity chromatography. *C*, pSASTISK was mixed with the tryptic digest of ^{32}P-phosphorylated Kv1.2-WT-myc and separated by electrophoresis and chromatography. Synthetic phosphopeptide (*left*) and ^{32}P-labeled phosphopeptides (*right*) were visualized by ninhydrin staining and autoradiography, respectively. + indicates the origin.

tryptic peptides by immobilized metal affinity chromatography that detected a single major radioactive peak at fractions 18–23 (Fig. 3*B*).

The Kv1.2 Phosphopeptide Co-migrates with the Synthetic Peptide pSASTISK—Based on canonical PKA phosphorylation consensus sequences (24), Ser-449 (Fig. 1) presented as an excellent candidate site. Assuming complete digestion with trypsin, Ser-449 would be expected to be the first serine in the peptide SASTISK. Tryptic digests of ^{32}P-labeled Kv1.2-WT-myc were, therefore, mixed with pSASTISK and separated. Fig. 3*C* shows that the tryptic Kv1.2-WT phosphopeptide migrated to the same position as the monophosphorylated synthetic peptide, consistent with phosphorylation at one serine residue(s) between 449 and 455.

A

B
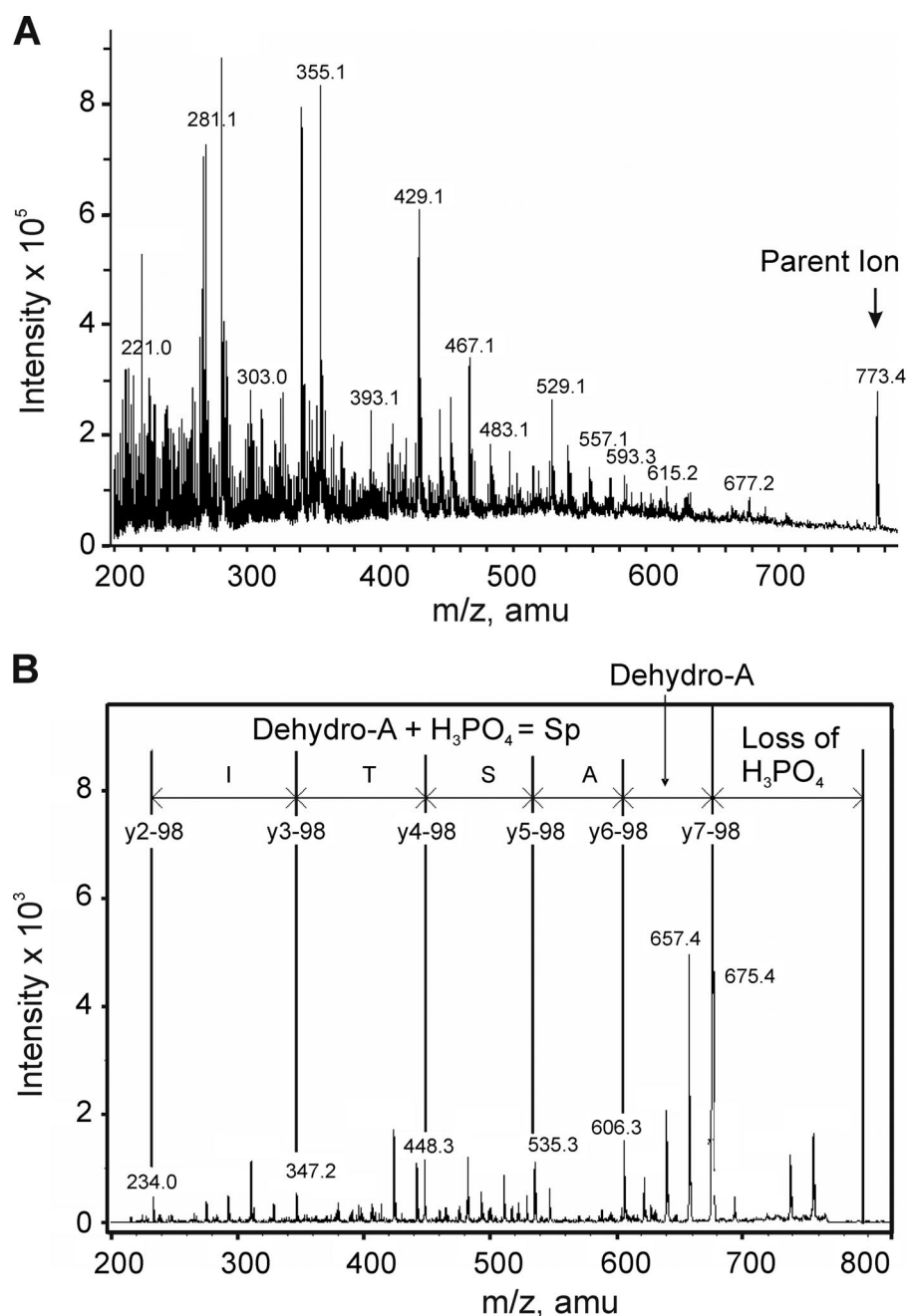
FIGURE 4. **Identification of Ser-449 of Kv1.2 as a site of phosphorylation after *in vitro* PKA treatment.** ^{32}P-Labeled tryptic peptides of Kv1.2-WT-myc after *in vitro* PKA treatment were partially purified on a C18 column and analyzed by mass spectrometry. *A*, ion trap full scan MS spectrum of Kv1.2-myc tryptic digest showing a major phosphopeptide with *m/z* 773.4. *B*, MS/MS spectrum resulting from isolation and collision-induced fragmentation of the singly charged *m/z* 773.4 precursor ion. The sequence of the *m/z* 773.4 ion shown is based on a y-ion series (separated by *vertical lines*). amu, atomic mass units; *Sp*, phosphoserine.

ion spectrum shown in Fig. 4*B*. Phosphorylation was detected by the M-98 peak corresponding to the loss of H_3PO_4 (*m/z* 675.4) and supported by the detection of a residue mass consistent with the presence of dehydroalanine at *m/z* 606.5 (arising from the β-elimination of phosphate from serine residues). The peptide sequence was determined by MASCOT to correspond to pSASTISK and manually verified. The synthetic phosphopeptide, pSASTISK, generated an identical fragmentation pattern (data not shown).

Mass spectrometry was employed to identify residues of Kv1.2-WT and Kv1.2-S449A exhibiting phosphorylation *in situ*. Kv1.2-WT was immunoprecipitated from HEK 293 cells in control conditions and after treatment with 8-Br-cAMP (1 mM) for 30 min and subjected to tryptic digestion and LC-MS/MS analysis. The *m/z* 773.5 ion was detected in control and 8-Br-cAMP-treated cell samples of Kv1.2-WT, and the product ion spectra shown in Figs. 5, *A* and *B*, respectively, were consistent with those obtained in the *in vitro* phosphorylation experiments.

A MIDAS approach was used to determine whether additional sites on Kv1.2-WT and Kv1.2-S449A were also phosphorylated *in situ*. The enhanced signal-to-noise ratio associated with this approach allows for more sensitive detection of phosphopeptides in low abundance proteins compared with LC-MS/MS (35). Tryptic peptides derived from all cytoplasmic domains of Kv1.2-WT (Fig. 1) and Kv1.2-S449A of control and 8-Br-cAMP-treated HEK 293 cells were considered in this analysis. Phosphorylation of

Identification of the in Vitro PKA Phosphorylation Site as Ser-449—The high hydrophilicity of ^{32}P-labeled tryptic peptide permitted partial purification using a reverse phase C18 column, with the flow-through examined by MALDI-TOF MS. This approach identified a major peptide of *m/z* 773.4 corresponding to the predicted protonated mass of the tryptic peptide containing phosphorylated Ser-449 (*i.e.* pSASTISK). This species was visible in direct infusion nanospray experiments, as shown in Fig. 4*A*. The singly charged *m/z* 773.4 ion was selected for MS/MS analysis, and fragmentation produced the product

Ser-449 (data not shown) and two additional residues, Ser-440 and Ser-441 (at retention times of 23 and 24 min, respectively; Fig. 6, *A* and *B*), was identified in Kv1.2-WT of control and 8-Br-cAMP-treated cells. This result is similar to the pattern previously detected by Yang *et al.* (26), but contrary to their observations, we did not detect phosphorylation of Ser-434. The Ser-440 and Ser-441 sites had 532.8 > 488.8 transitions (2+ charged state), indicating a loss of H_3PO_4. Associated MASCOT and manual product ion scans confirmed these phosphorylated tryptic peptides to be IPpSSPDLKK and IPSp-
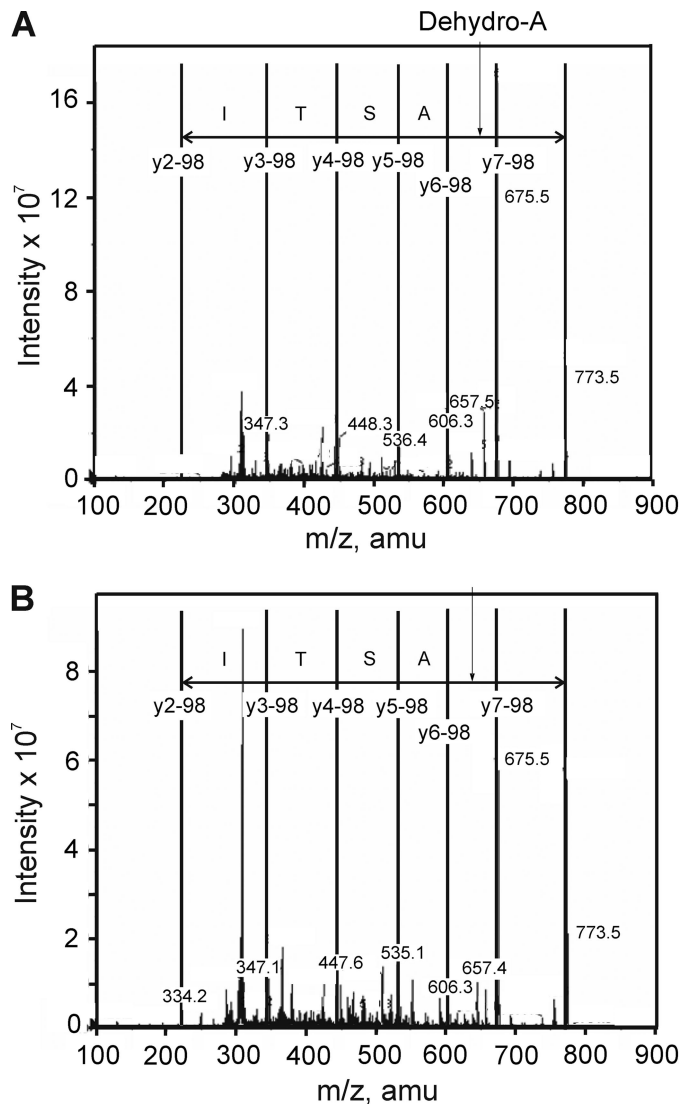
FIGURE 5. **Confirmation of *in situ* phosphorylation of Kv1.2 at Ser-449.** *A*, MS/MS spectrum resulting from isolation and collision-induced fragmentation of the singly charged *m/z* 773.4 precursor ion obtained from ion trap full scan MS spectrum of control HEK 293 cell Kv1.2-WT-myc tryptic digest. The sequence of the *m/z* 773.4 ion shown is based on a y-ion series (separated by *vertical lines*). *B*, MS/MS spectrum of the singly charged *m/z* 773.4 precursor ion obtained from ion trap full scan MS spectrum of 8-Br-cAMP-treated HEK 293 cell Kv1.2-WT-myc tryptic digest. The sequence is as indicated in *A*. *amu*, atomic mass units.

SPDLKK (*i.e.* Ser-440 and Ser-441, respectively; Fig. 6). We also detected Ser-440 and Ser-441 phosphorylation in control and 8-Br-cAMP-treated HEK 293 cells expressing Kv1.2-S449A (data not shown). Significantly, no additional phosphorylated tryptic fragments were identified after 8-Br-cAMP treatment compared with control conditions for HEK 293 cells expressing Kv1.2-WT or Kv1.2-S449A.

Effect of Mutations on in Vitro ^{32}P Incorporation into Kv1.2—The effect of mutating Ser-440, Ser-441, and Ser-449 on *in vitro* ^{32}P incorporation was examined. Fig. 7*A* shows an autoradiogram of ^{32}P incorporation and anti-Myc immunoblot of Kv1.2-WT, -T46A, -S449A, -S449D, the double mutant Kv1.2-S440A/S441A, and the triple mutant Kv1.2-S440A/S441A/S449A. ^{32}P incorporation for each mutant expressed as a % of that for Kv1.2-WT is shown in Fig. 7*B*. The T46A and double S440A/

S441A mutations were without effect on ^{32}P incorporation. The S449A, S449D, and triple S440A/S441A/S449A mutations significantly reduced ^{32}P incorporation to 25.8 ± 6.7, 31.8 ± 6.6, and $35.1 \pm 3.8\%$, respectively, of wild-type protein, but incorporation was not abolished. For this reason we performed phosphopeptide mapping on ^{32}P-labeled Kv1.2-S449A after mixing the tryptic digest with synthetic pSASTISK (Fig. 7*C*). The peptides migrated to the same position, but visualization of ^{32}P-labeled peptide required an exposure time of 4 weeks compared with just 3 days for Kv1.2-WT peptide (Fig. 3*C*). This is consistent with a much lower efficiency of ^{32}P incorporation.

Synthetic Kv1.2 Peptide Is a Substrate for PKA—Synthetic peptide KKSRSASTISK corresponding to residues 445–455 of Kv1.2 was tested as a substrate using [γ-^{32}P]ATP and varied cPKA concentrations. Phosphorylation was dependent on cPKA concentration and did not exceed 1 mol of phosphate/mol of peptide (Fig. 8*A*). Kemptide (LLRRASLG) and the Ser-449 null peptide, KKSRAASTISK, were tested as positive and negative controls, respectively. Kemptide was phosphorylated to a stoichiometry of ~1 mol/mol at all concentrations of cPKA tested, whereas the null peptide showed low, non-stoichiometric levels of ^{32}P incorporation even at 5 μg/ml cPKA (Fig. 8*A*). These results indicate that there is one principal site of phosphorylation between residues 445–455 but that phosphorylation at substoichiometric levels can occur at adjacent residues in the absence of Ser-449.

The kinetics of PKA phosphorylation were examined using KKSRSASTISK, Kemptide, and the Ser-449 null peptide. PKA phosphorylation of KKSRSASTISK and Kemptide demonstrated substrate concentration dependence (Fig. 8*B*) that obeyed Michaelis-Menten kinetics; K_m and V_{max} values calculated using alternative methods are shown in Table 1. The negligible ^{32}P incorporation into the null peptide precluded determination of K_m and V_{max} values.

Effect of Mutation on PKA-dependent Alterations in Kv1.2 Current Amplitude—Fig. 9*A* shows representative families of whole-cell currents due to Kv1.2-WT and -S449A mutant expression obtained using step depolarizations to between −80 and +30 mV before (Control) and after 8-Br-cAMP (1 mM) treatment. Current density, activation and deactivation kinetics, and voltage dependence of activation of Kv1.2-WT and -S449A currents in control conditions were identical (Table 2). An increase in Kv1.2-WT current amplitude was apparent within 5 min of 8-Br-cAMP addition and reached a stable level in all cells within 10 min (assessed by repetitive application of steps from −60 to +20 mV at 15-s intervals; Fig. 10*A*). In contrast, no change was observed for Kv1.2-S449A current in >10 min (Fig. 10*A*). Comparison of normalized I-V relations showed that 8-Br-cAMP increased Kv1.2-WT current at all voltages positive to −40 mV, but S449A was unaffected by PKA activator treatment (Fig. 9*A*).

VSM Kv1-containing K_{DR} channels were previously shown to be phosphorylated by PKA under basal conditions (10, 12). Here, this was assessed by bath application of the membrane-permeant analog, Rp-CPT-cAMPS, which competes with cAMP at the regulatory subunit of PKA (Figs. 9*B* and 10*B*). The representative whole-cell currents and mean normalized I-V relations in Fig. 9*B* show that Kv1.2-WT, but not
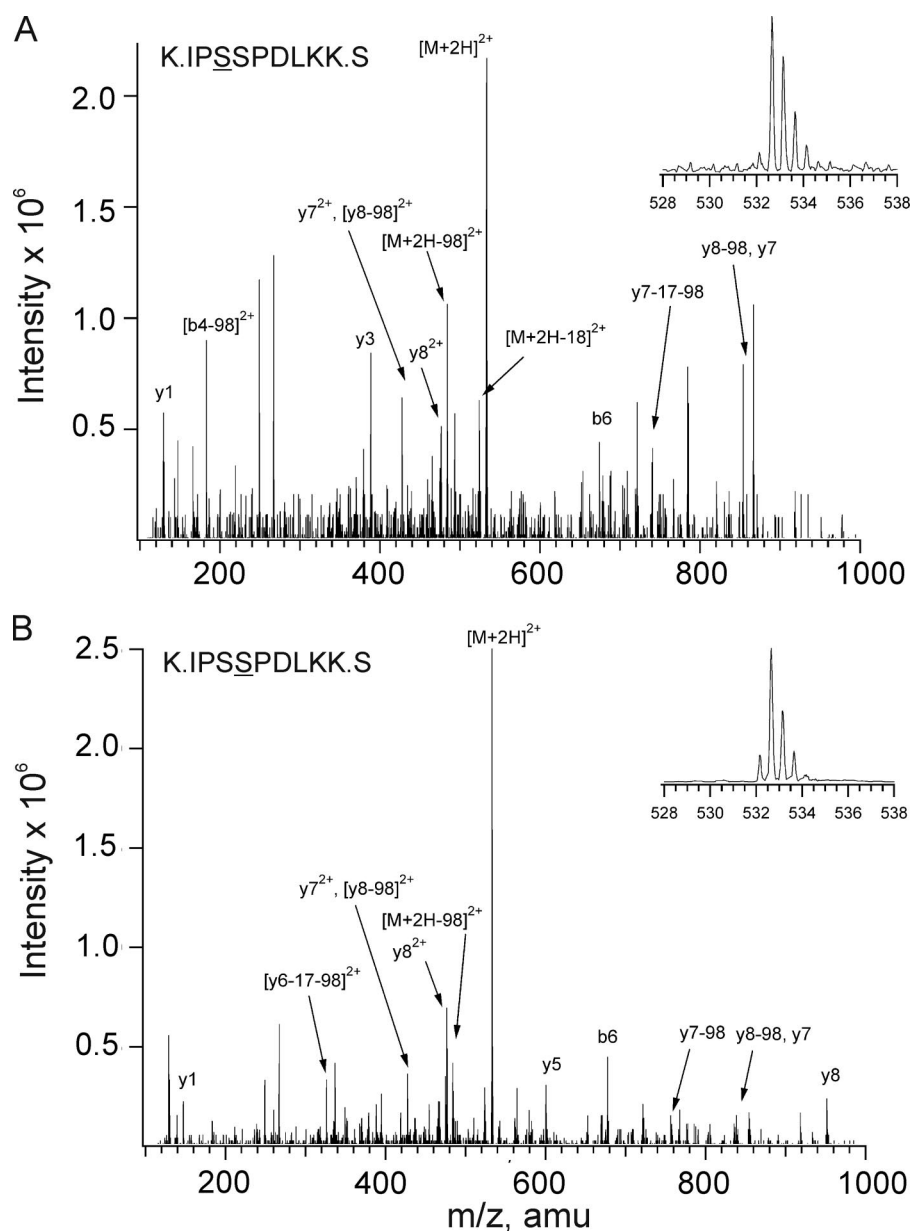
FIGURE 6. **Identification of Ser-440 and Ser-441 as additional sites of *in situ* phosphorylation of Kv1.2.** MS/MS spectra obtained from MIDAS analysis of tryptic digest of control HEK 293 cell Kv1.2 with ion assignments based on Mascot annotation and manual validation. *A*, spectrum of early eluting phosphopeptide. *B*, spectrum of late eluting phosphopeptide. *Insets* in each panel represent enhanced resolution scans of the respective precursor ions (*m/z* 532.7). Identical spectra were obtained for 8-Br-cAMP-treated cells expressing Kv1.2-WT. *amu*, atomic mass units.

dialysis with Rp-CPT-cAMPS was similar to that observed for bath applied analog, as was the lack of change in Kv1.2-S449A current (Fig. 10, *B* and *C*). Fig. 10*D* shows that subsequent application of 8-Br-cAMP to cells dialyzed with Rp-CPT-cAMPS failed to cause an increase in Kv1.2-WT current amplitude within the time required for Kv1.2-WT cells not exposed to Rp-CPT-cAMPS to exhibit a significant increase in current (Fig. 10*A*).

The effect of dialysis with cPKA (50 nM) was assessed for untransfected HEK 293 cells and cells expressing Kv1.2-WT, Kv1.2-S449A, Kv1.2-S449D, Kv1.2-S440A/S441A, and Kv1.2-S440A/S441A/S449A channels. Figs. 11, *A–F*, show representative whole-cell currents evoked by 5-s voltage ramps between −80 and +40 mV to assess the quasi-steady state I-V relation for each channel type immediately after membrane rupture and after the indicated times of dialysis with cPKA. Current amplitude was negligible in untransfected cells, and no difference in initial current density measured at +40 mV immediately after membrane rupture was apparent for wild-type and mutant channel constructs employed in these experiments (Fig. 11*G*) (cell capacitance was 28.9 ± 1.4 pF; *n* = 27). A similar lack of difference in initial current density was apparent when all cells exhibiting successful membrane rupture were considered, including those where the recording time was only briefly maintained (*i.e.* <0.5–1 min). In this case, the density of the S449D, double, and triple mutant currents were 203 ±

Kv1.2-S449A, current amplitude was reduced after Rp-CPT-cAMPS (25 μM) treatment. A stable reduction in Kv1.2-WT current was apparent within 6 min of Rp-CPT-cAMPS treatment, but current due to the mutant channels showed no change in amplitude in this time period (Fig. 10*B*).

To control for non-PKA-mediated effects of 8-Br-cAMP, this analog was also applied after dialysis with pipette solutions containing Rp-CPT-cAMPS. Fig. 10*C* shows that dialysis with Rp-CPT-cAMPS reduced Kv1.2-WT, but not Kv1.2-S449A, amplitude over time after membrane rupture (assessed by repetitive application of steps from −60 to +20 mV every 15 s immediately after membrane rupture). The fractional change in end-pulse Kv1.2-WT current amplitude at +20 mV due to

42, 180 ± 31, and 402 ± 245 pA/pF (12, 14, and 5 cells), respectively, and not different from that of Kv1.2-WT at 309 ± 129 pA/pF (7 cells).

A stable increase in Kv1.2-WT current amplitude was detected by 5–8 min of dialysis with cPKA, but no change in current was detected over an identical time in the absence of the kinase (Fig. 11, *A* and *B*). Whole-cell currents due to the double Kv1.2-S440A/S441A mutant were also increased by dialysis with cPKA, but no change in current was detected for the Kv1.2-S449A, -S449D, or triple -S440A/S441A/S449A mutant channels (Fig. 11, *C–F*). Fig. 12*H* indicates that on average, only the Kv1.2-WT and double Kv1.2-S440A/S441A mutant channels exhibited a significant fractional increase in current at +40 mV during dialysis with cPKA.
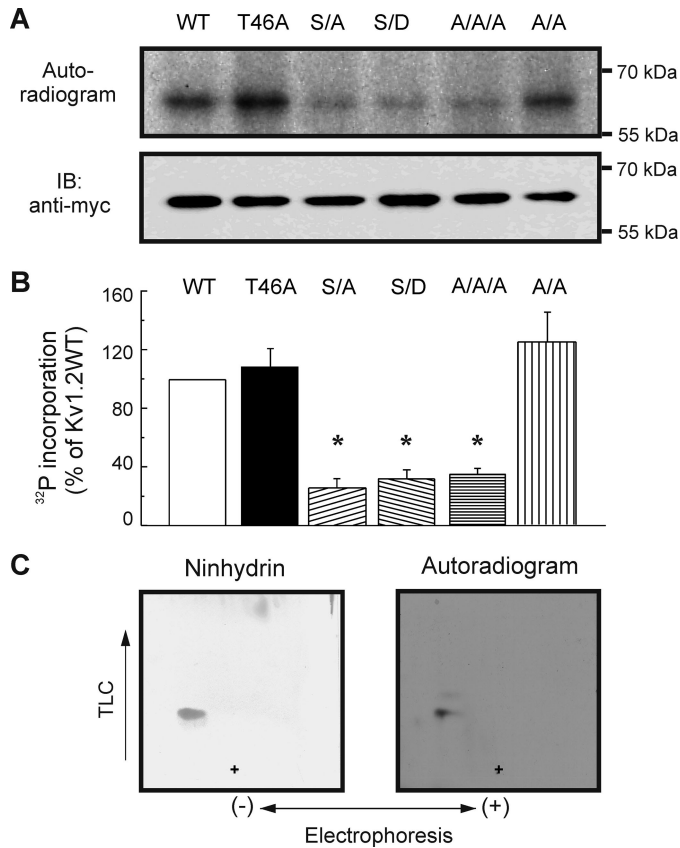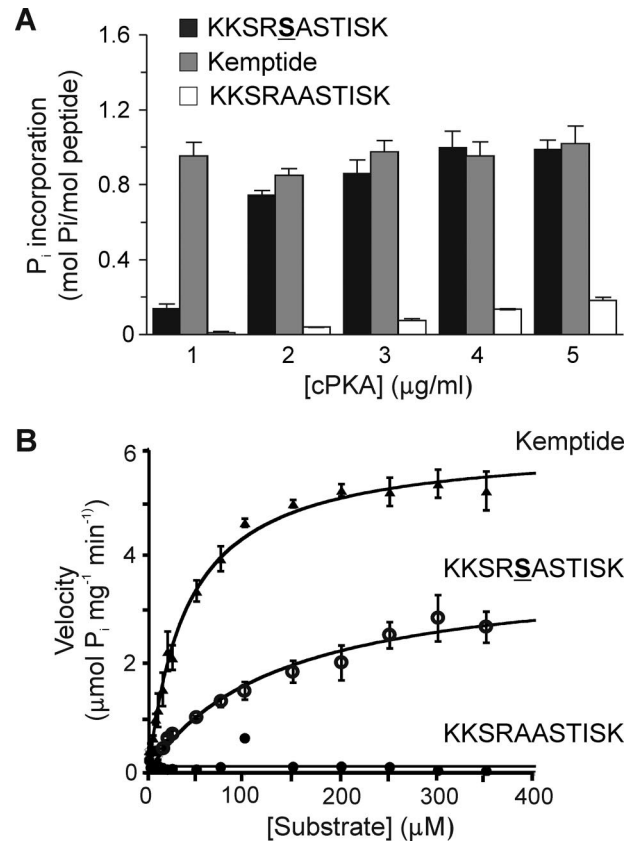
FIGURE 7. **Quantitative analysis of ³²P incorporation by wild-type and mutant Kv1.2 constructs during in vitro PKA treatment.** *A*, levels of ³²P incorporation and protein in anti-Myc immunoprecipitates of tagged Kv1.2-WT (*WT*), -T46A, -S449A (*S/A*), -S449D (*S/D*), -S440/S441A (*A/A*), and -S440A/S441A/S449A (*A/A/A*) channels after *in vitro* phosphorylation by PKA were detected by autoradiography (*upper panel*) and immunoblotting (*IB*) with anti-Myc (*lower panel*), respectively. *B*, ³²P incorporation relative to total protein was determined by densitometric analysis and expressed as a % of the value for Kv1.2-WT. Data are the means ± S.E. (*n* = 5). *Asterisks* indicate significant difference ($p < 0.05$) from Kv1.2-WT by analysis of variance followed by the Bonferroni post-hoc test. *C*, co-migration of synthetic pSASTISK and ³²P-labeled Kv1.2-S449A-myc mutant tryptic phosphopeptides was detected by ninhydrin staining and autoradiography. Data are representative of three experiments. + indicates the origin.

FIGURE 8. **Stoichiometric and kinetic analysis of PKA-catalyzed ³²P incorporation by synthetic peptide.** Synthetic peptide KKSR**S**ASTISK, corresponding to amino acid residues 445–455 of Kv1.2 and containing the putative PKA site Ser-449, was compared as a substrate to LLRRASLG (Kemptide) (positive control) and KKSRAASTISK (corresponding to the sequence of Kv1.2-S449A mutant, negative control). *A*, fixed concentrations of each peptide (50 μM) were treated with [γ-³²P]ATP and cPKA (1.0–5.0 μg/ml), and ³²P incorporation was quantified by Čerenkov counting. Data are the means ± S.E. of three independent experiments carried out in triplicate. *B*, cPKA activity was determined by quantification of ³²P incorporation into KKSR**S**ASTISK, Kemptide, and KKSRAASTISK peptides during the linear phase of the reaction (*t* = 1.5 min). Enzyme velocities were plotted against substrate concentration and fitted to the Michaelis-Menten equation to obtain K_m and V_{max} values.

A final set of experiments was conducted using excised, inside-out membrane patches under symmetrical 140/140 mM KCl recording conditions (*i.e.* with 5 mM ATP, 1 mM EGTA and no added Ca^{2+} in the bath). The patches were stepped from a transmembrane potential of −60 to +40 mV for 250 ms at 15-s intervals, and the change in current was recorded in the control solution or in the presence of cPKA (50 nM). A stable increase of ~4-fold in Kv1.2-WT current was detected by 4 min in three patches exposed to cPKA, but a slight decrease in amplitude was detected for three patches under control conditions by 4 min (Fig. 12).

DISCUSSION

Modulation of VSM Kv1 channel activity by cellular signaling pathways involving PKA activation is well known (10, 12, 13, 21, 22), but the molecular basis of this regulation is unclear. This study indicates that whole-cell current due to heterologous expression of Kv1.2, a component of VSM Kv1 channels (4–6, 28), is increased by PKA-catalyzed phospho-

rylation of Ser-449 but not Thr-46 (23) or Ser-440 and Ser-441 (26). This conclusion is based on the following. 1) Phosphoamino acid analysis of *in vitro* phosphorylated Kv1.2 protein showed phosphorylation occurred exclusively at serine residues, 2) mutation of Ser-449, but not Thr-46 or Ser-440 and Ser-441, significantly reduced *in vitro* PKA-catalyzed ³²P incorporation by Kv1.2, 3) phosphopeptide mapping revealed one major PKA ³²P-labeled phosphopeptide for Kv1.2-WT and T46A, 4) *in vitro* phosphorylation assays indicated that a synthetic peptide with a sequence equivalent to that of the tryptic peptide containing Ser-449 was stoichiometrically phosphorylated by PKA with K_m and V_{max} values comparable with those reported for other PKA substrates (36), 5) sequencing of Kv1.2-WT protein by LC-MS/MS identified Ser-449 as the residue phosphorylated by PKA *in vitro*, 6) analysis of intracellular Kv1.2-WT tryptic peptides by a combination of LC-MS/MS and MIDAS showed *in situ* phosphorylation at Ser-440, Ser-441, and Ser-449 under control conditions. No additional sites of *in situ* phosphorylation were detected after treatment with 8-Br-

TABLE 1

Kinetic parameters of cPKA-catalyzed phosphorylation of KKSRSASTISK, Kemptide, and KKSRAASTISK peptides

Substrate concentrations used were 1, 2.5, 5, 7.5, 10, 15, 20, 25, 50, 75, 100, 150, 200, 250, 300, and 350 μM; cPKA and ATP were 2.0 μg/ml and 0.2 mM, respectively. K_m and V_{max} values were calculated by linear regression analysis of Lineweaver-Burk or Eadie-Hofstee plots or by Michaelis-Menten analysis (Fig. 8*B*). Values are expressed as the mean $\pm$ S.E. of three experiments performed in triplicate. $-$ indicates no ^{32}P incorporation.

Analysis	Peptide	K_m	V_{max}	K_m/V_{max}
		μM	$\mu mol\ P_i\ mg^{-1}\ min^{-1}$	
Michaelis-Menten	KKSRSASTISK	133.8 $\pm$ 30.0	3.8 $\pm$ 0.4	35.2
	Kemptide	39.9 $\pm$ 2.8	6.1 $\pm$ 0.1	6.5
	KKSRAASTISK	$-$	$-$	$-$
Lineweaver-Burk	KKSRSASTISK	101.8 $\pm$ 26.7	2.7 $\pm$ 0.6	37.7
	Kemptide	35.1 $\pm$ 3.6	5.8 $\pm$ 0.2	6.1
	KKSRAASTISK	$-$	$-$	$-$
Eadie-Hofstee	KKSRSASTISK	98.7 $\pm$ 25.7	3.1 $\pm$ 0.09	38.1
	Kemptide	34.9 $\pm$ 2.7	5.8 $\pm$ 0.1	6.0
	KKSRAASTISK	$-$	$-$	$-$

cAMP; and 7) modulation of Kv1.2-WT by PKA activation with 8-Br-cAMP by PKA inhibition with Rp-CPT-cAMPS or by intracellular dialysis with cPKA were prevented by mutation of Ser-449 but not by mutation of Ser-440 and Ser-441. Taken together, these findings provide compelling evidence that phosphorylation of Ser-449 underlies the increase in activity of recombinant Kv1.2 channels expressed in HEK 293 cells due to PKA.

Phosphorylation of brain Kv1.2 and recombinant Kv1.2 channels in heterologous cells was previously detected using tandem MS (26, 27). Specifically, phosphorylation at Ser-440 and Ser-441 was identified for rat, mouse, and human brain (phosphorylation at Ser-434 was also apparent in rat and mouse brain) (26), whereas phosphorylation of Ser-440, Ser-441, and/or Ser-449 was detected in Kv1.2 expressed in HEK 293 or COS-1 cells (26, 27) (HEK 293 cells also showed Ser-434 phosphorylation (26)). Our LC-MS/MS and MIDAS analysis of *in situ* Kv1.2 using HEK 293 cells in the absence and presence of 8-Br-cAMP confirmed the presence of phosphorylation at Ser-440, Ser-441, and Ser-449 but not Ser-434. Yang *et al.* (26) employed stable isotope-labeling with amino acids in cell culture (SILAC) analysis for quantification of Ser-440 and Ser-441 phosphorylation levels in internal *versus* surface membrane populations of Kv1.2, but this approach was not successful for quantification of Ser-449 phosphorylation. We attempted to quantify Ser-449 phosphorylation levels in control and 8-Br-cAMP-treated cells using a proteolytic ^{18}O-labeling approach. However, this approach was also not successful due to the loss of labeling through back-exchange.

Alternatively, the relevance of Ser-440, Ser-441, and Ser-449 to the modulation of Kv1.2 channel activity by PKA was examined here by whole-cell patch clamp analysis. Our data indicate that Ser-449, but not Ser-440 and Ser-441, is important for modulation of the Kv1.2 channel activity by PKA. Treatment with 8-Br-cAMP or Rp-CPT-cAMPS increased and decreased, respectively, the amplitude of Kv1.2-WT but had no effect on the amplitude of Kv1.2-S449A current. Similarly, dialysis with cPKA increased the amplitude of Kv1.2-WT and Kv1.2-S440A/S441A, but not Kv1.2-S449A, Kv1.2-S449D, or Kv1.2-S440A/S441A/S449A current. We do not attribute the changes in current amplitude to insertion or withdrawal of channels from the surface membrane, as a stable increase in Kv1.2-WT current amplitude was observed within 4 min in excised, inside-out patches exposed to cPKA in the presence of ATP but not in

patches treated with identical solution lacking cPKA. It is highly unlikely that cPKA altered surface expression in this context as the experiments were performed using low (1–10 nM) Ca^{2+} bath solution that would be expected to prevent vesicle endocytosis or fusion with the plasma membrane. Also, the previously described decrease in surface expression due to PKA (27) would not seem relevant. This would reduce Kv1.2 current amplitude rather than causing the increase reported here. Huang *et al.* (23) previously tested for modulation of the S449A mutant channel by PKA. In direct contrast to our findings, enhancement of current amplitude in *Xenopus* oocytes after β-adrenoreceptor activation or application of cPKA was unaffected by the S449A mutation. The reason(s) for this discrepancy is not clear. It is possible that the Ser-449 is not available for phosphorylation when Kv1.2 is expressed in *Xenopus* oocytes.

We found that dialysis with Rp-CPT-cAMPS prevented the 8-Br-cAMP-induced increase in Kv1.2-WT current. This implies that the change in current was due to PKA rather than a nonspecific side effect of 8-Br-cAMP, as the inactive analog Rp-CPT-cAMPS competes with cAMP for binding to the regulatory subunit of PKA. That Kv1.2-WT, but not Kv1.2-S449A, current amplitude was reduced by bath treatment or dialysis with Rp-CPT-cAMPS implies that the channels must have a basal level of phosphorylation at Ser-449. This view is consistent with our *in situ* LC-MS/MS and MIDAS analysis as well as previous proteomic studies of Kv1.2 expressed in HEK 293 and COS-1 cells that detected the presence of basal phosphorylation of Ser-449 in heterologous cell types (26, 27). The presence of basal, PKA-mediated phosphorylation was also previously inferred for native VSM Kv1 channels containing Kv1.2 based on a reduction of basal whole-cell current by PKA inhibitor peptide (10) and recovery of single channel activity from rundown in the presence of cPKA (12). Interestingly, basal phosphorylation of Ser-449 was not detected for brain Kv1.2 (26).

Yang *et al.* (26) found that the S449A mutation resulted in a reduction in phosphorylation at Ser-440 and Ser-441 and proposed that phosphorylation at Ser-449 might be required for subsequent phosphorylation at Ser-440 and Ser-441. Although our experiments did not directly assess this issue, the lack of effect of PKA stimulation on current amplitude of the phosphomimetic mutant, Kv1.2-S449D, implies that sequential phosphorylation at Ser-449 followed by Ser-440/Ser-441 phosphorylation is not involved in PKA-dependent modulation of Kv1.2
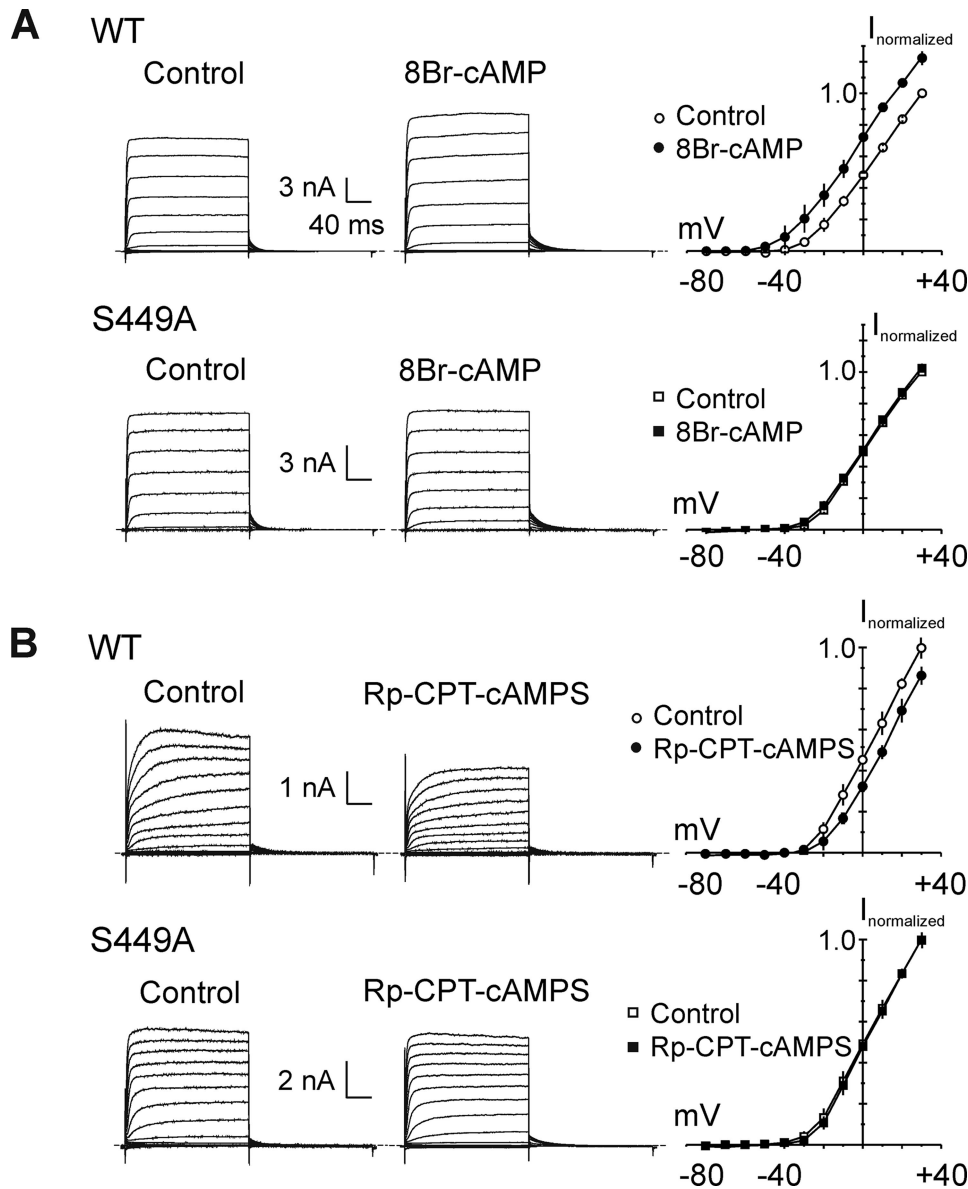
FIGURE 9. S449A mutation prevents modulation of Kv1.2 current amplitude by PKA activation or inhibition. *A*, representative families of whole-cell currents recorded during 200-ms pulses between −80 and +30 mV in 10-mV steps from HEK 293 cells transiently expressing Kv1.2-WT (*WT*; n = 4) or Kv1.2-S449A (*S449A*; n = 4) before (*Control*) and after 8-Br-cAMP (1 mM; *8-Br-cAMP*) treatment and the corresponding mean (±S.E.) fractional I-V relations in control (*open circles*) and 8-Br-cAMP (*closed circles*) (*i.e.* plots are the average values of end pulse current at each voltage ± 8-Br-cAMP normalized to value in control condition at +30 mV in each cell). Mean fractional current in 8-Br-cAMP was significantly greater than that in control condition at all voltages positive to −40 mV for Kv1.2-WT (*p* < 0.05; unpaired Student's *t* test) but not different for Kv1.2-S449A. *B*, representative families of Kv1.2-WT (*WT*; n = 4) or Kv1.2-S449A (*S449A*; n = 3) whole-cell currents and corresponding mean ± S.E. fractional I-V relations (as in *A*) before (*Control*) and after Rp-CPT-cAMPS (25 μM; *Rp-CPT-cAMPS*) treatment. Mean fractional current in Rp-CPT-cAMPS was significantly reduced compared with control conditions at all voltages positive to −20 mV for Kv1.2-WT (*p* < 0.05; unpaired Student's *t* test) but not different for Kv1.2-S449A.

channel activity. Moreover, dialysis with cPKA increased Kv1.2-S440A/S441A current amplitude by a similar increment as that observed for Kv1.2-WT channels and was without effect on the Kv1.2-S440A/S441A/S449A mutant. This implies that phosphorylation at Ser-440 and Ser-441 are not required for PKA-dependent increases in Kv1.2 current amplitude. Yang *et al.* (26) also indicated that Ser-440, Ser-441, and Ser-449 phosphorylation may be required for trafficking to the surface membrane. We did not find any difference in current density for wild-type and mutant channels in our analysis.

Our *in vitro* analysis of PKA-catalyzed ^{32}P incorporation revealed that the level of Kv1.2-S449A phosphorylation was reduced by ∼75% compared with that of Kvl.2-WT. This indicates that Ser-449 is a principal site of *in vitro* PKA-catalyzed phosphorylation. However, ^{32}P incorporation was not completely abolished by this mutation. One explanation for this result would be that phosphorylation at Ser-440 and/or Ser-441 contributes to the total observed Kv1.2 phosphorylation. However, this is apparently not the case, as ^{32}P incorporation by the double S440A/S441A and triple S440A/S441A/S449A mutant channels was similar to that of Kv1.2-S449A.

Alternatively, the residual ^{32}P incorporation by Kv1.2-S449A could result from substoichiometric phosphorylation at an adjacent serine residue when Ser-449 is replaced with an alanine. Our results support this interpretation. 1) *In vitro* cPKA-catalyzed phosphorylation of the synthetic peptide, KKSRSAS-TISK, resulted in a stoichiometry of

TABLE 2

Comparison of the biophysical properties of Kv1.2-WT and Kv1.2-S449A

Parentheses indicate the number of cells. Current density and activation time constants were measured from whole-cell currents elicited by a step depolarization from −60 to +20 mV. Deactivation time constants were measured from tail currents elicited by a step to −50 mV from +20 mV. Current density, time constants, and $V_{0.5}$ for activation of Kv1.2-WT and -S449A were not significantly different (*p* > 0.05) by unpaired Student's *t* test.
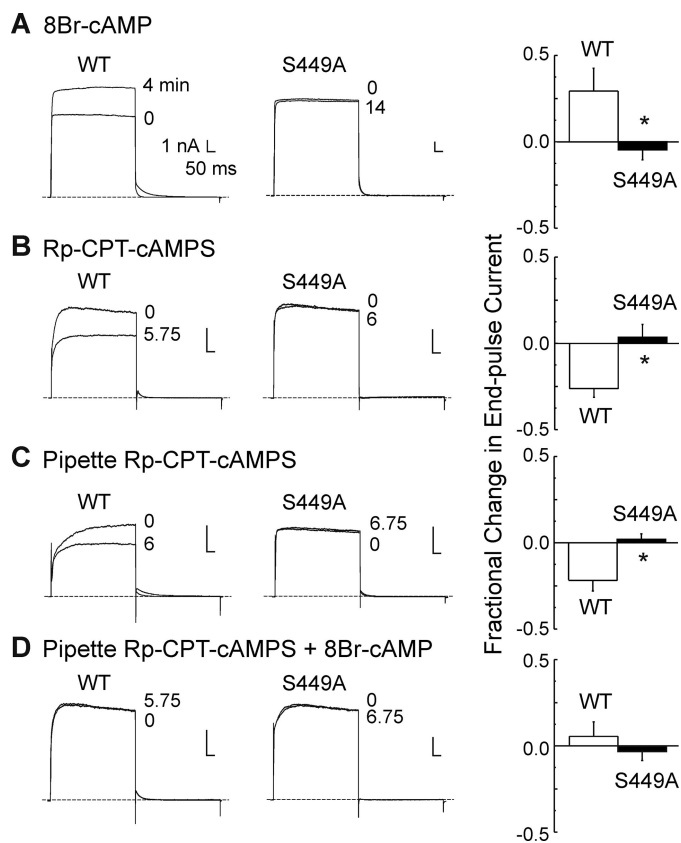
	Current density at +20 mV	Activation time constant		Deactivation time constant		Activation $V_{0.5}$
		τ_1	τ_2	τ_1	τ_2	
	pA/pF	*ms*	*ms*	*ms*	*ms*	*ms*
Kv1.2-WT	212.9 ± 50.2 (15)	0.29 ± 0.05 (6)	0.90 ± 0.17 (6)	10.0 ± 1.6 (10)	34.2 ± 5.7 (10)	−16.4 ± 3.9 (5)
Kv1.2-S449A	187.5 ± 30.9 (11)	0.5 ± 0.1 (6)	1.5 ± 0.5 (6)	9.6 ± 1.4 (9)	33.5 ± 5.1 (9)	−14.4 ± 2.0 (4)

A 8Br-cAMP

B Rp-CPT-cAMPS

C Pipette Rp-CPT-cAMPS

D Pipette Rp-CPT-cAMPS + 8Br-cAMP

FIGURE 10. **Time dependence of Kv1.2 current amplitude modulation by PKA activation and inhibition and effect of Rp-CPT-cAMPS on basal and 8-Br-cAMP-induced increase in Kv1.2 current.** *A*, representative whole-cell currents during 250-ms voltage steps to +20 mV (applied at 15-s intervals) recorded before (0 min) and when a stable change in current amplitude was detected at 4 min for Kv1.2-WT (*WT*; *n* = 3) and at 14 min for Kv1.2-S449A (*S449A*; *n* = 4) as well as the mean (±S.E.) fractional change in Kv1.2-WT (*n* = 3) and S449A (*n* = 4) end pulse current (*n* = 4) due to treatment with 8-Br-cAMP (1 mM). *B*, representative whole-cell currents (evoked by voltage protocol in *A*) recorded before (0 min) and when a stable change in current amplitude was detected at 5.75 min for Kv1.2-WT (*WT*) and at 6 min for Kv1.2-S449A (*S449A*) as well as the mean (±S.E.) fractional change in Kv1.2-WT (*n* = 4) and S449A (*n* = 3) end pulse current due to bath treatment with Rp-CPT-cAMPS (25 μM). *C*, representative Kv1.2-WT and Kv1.2-S449A whole-cell currents (evoked by protocol in *A*) recorded immediately after membrane rupture (0 min) and after 6 and 6.75 min, respectively, of dialysis with Rp-CPT-cAMPS (25 μM) as well as the mean (±S.E.) fractional change in Kv1.2-WT (*n* = 4) and S449A (*n* = 3) end pulse current due to Rp-CPT-cAMPS. *D*, representative Kv1.2-WT and Kv1.2-S449A whole-cell currents (evoked by protocol in *A*) before (0) and after 5.75 and 6.75 min of treatment with 8-Br-cAMP (1 mM), respectively, after dialysis with Rp-CPT-cAMPS (25 μM) as well as the mean (±S.E.) fractional change in end pulse current (*n* = 3 in each group) due to 8-Br-cAMP in the presence of Rp-CPT-cAMPS. The *asterisks* in *A–D* indicate values for S449A mutant were significantly different from Kv1.2-WT by unpaired Student's *t* test (*p* < 0.05).

A

B

C

D

E

F

G

H

FIGURE 11. **Modulation of whole-cell Kv1.2 current by cPKA requires Ser-449.** *A–F*, representative whole-cell currents due to wild-type (*WT*) and mutant Kv1.2 (*S449A*, *S449D*, *S440A/S441A*, and *S440A/S441A/S449A*) constructs evoked by 5-s voltage ramps from −80 to +40 mV (applied at 20-s intervals) immediately after membrane rupture (0 min) and after the indicated times of dialysis with control pipette solution (*panel A*; Kv1.2WT (*WT (no cPKA)*) or solution with cPKA (50 nM; *B–F*). The second tracing in each panel represents the stable level of current achieved after the indicated time. *G*, current density at +40 mV immediately after membrane rupture ±S.E. for untransfected HEK 293 cells (*UT*) and cells expressing Kv1.2-WT (*WT (no cPKA)* and WT), -S449A (*S/A*), -S449D (*S/D*), -S440A/S441A (*A/A*), or -S440A/S441A/S449A (*A/A/A*) (*n* values are as in *G*). *H*, mean fractional change in current at +40 mV ± S.E. (evoked by the ramp protocol indicated in *A*) for cells expressing wild-type or mutant Kv1.2 constructs after dialysis with control pipette solution (*WT (no cPKA)*) or solution containing cPKA (Kv1.2-WT (*WT*), S449A (*S/A*), S449D (*S/D*), S440A/S441A (*A/A*), and S440A/S441A/S449A (*A/A/A*)) (*n* values indicate *n* cells from >3 transfections). *H*, mean fractional change in current at +40 mV ± S.E. (evoked by the ramp protocol indicated in *A*) for cells expressing wild-type or mutant Kv1.2 constructs after dialysis with control pipette solution (*WT (no cPKA)*) or solution containing cPKA (Kv1.2-WT (*WT*), S449A (*S/A*), S449D (*S/D*), S440A/S441A (*A/A*), and S440A/S441A/S449A (*A/A/A*)). The *asterisks* indicate significantly different (*p* < 0.05) from Kv1.2-WT in the absence of PKA (*i.e. WT (no cPKA)*) determined by analysis of variance followed by the Bonferroni post-hoc test.

phosphorylation of ~1.0 mol of phosphate/mol of peptide. This is consistent with the presence of one principal phosphorylation site in the peptide. 2) The tryptic phosphopeptide derived from PKA-phosphorylated Kv1.2 co-migrated on a phosphopeptide map with monophosphorylated synthetic peptide, pSASTISK. pSASTISK corresponds to amino acid residues 449–455 of Kv1.2 and has a phosphate incorporated at the position equivalent to Ser-449. If the Kv1.2 tryptic peptide were phosphorylated on more than one residue, the additional charge(s) imparted by the phosphoryl group(s) would cause it to migrate to a different position compared with the phosphorylated synthetic peptide. The additional minor spots present in

the Kv1.2-WT and Kv1.2-T46A phosphopeptide maps (<5% total ^{32}P incorporation) are likely due to incomplete tryptic digestion, resulting in multiple phosphopeptides containing the same phosphorylated residue. This occurs when phosphorylated serine or threonine residues lie close to trypsin cleavage sites, as is the case for Ser-449 of Kv1.2 (31). 3) Phosphopeptide mapping of the Kv1.2-S449A tryptic digest produced one minor phosphopeptide that co-migrated with the tryptic phosphopeptide derived from Kv1.2-WT. [32]P incorporation into the peptide derived from the mutant channel was very low and at a substoichiometric level, as visualization by autoradiography
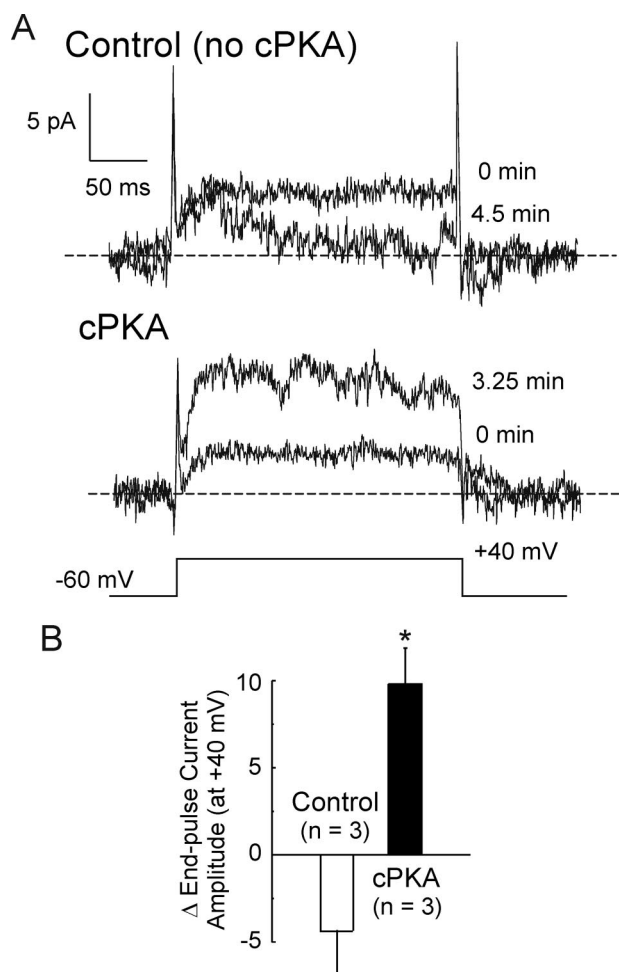
FIGURE 12. **Modulation of Kv1.2-WT current in excised, inside-out membrane patches by cPKA.** *A*, representative recordings of membrane patch current before (0 min) and after 4.5 and 3.25 min in control conditions and solutions containing 50 nM cPKA, respectively. *B*, average stable change in end-pulse current amplitude in control bath solution and in the presence of cPKA after 3.5–4.5 min (*n* = 3 patches each). The *asterisk* indicates significantly different from control, determined by unpaired Student's *t* test ($p < 0.05$).

required exposure to film for 4 weeks compared with 3 days for Kv1.2-WT.

Our identification of Ser-449 as a phosphorylation site for PKA in Kv1.2 is not consistent with the previously reported role for Thr-46 in mediating PKA stimulation of Kv1.2 (23). This discrepancy may reflect the different experimental approaches employed. Huang *et al.* (23) used site-directed T46V mutagenesis in combination with functional analysis of channels expressed in *Xenopus* oocytes by patch clamp methods. This approach does not provide a direct measure of channel phosphorylation. Moreover, interpreting the effects of modulating PKA activity on gating of Kv1.2-T46V channels is compromised by the fact that this mutation modifies channel function independent of phosphorylation (25). Specifically, structural analysis demonstrated that the γ-hydroxyl group of Thr-46 is buried from solvent and participates in an extensive hydrogen-bonding network involved in determination of channel stability (25). Mutation of this site alters channel gating, slowing the kinetics of activation and shifting the midpoint of activation by approximately +25 mV due to a stabilization of the closed state

(25). Therefore, the inability of PKA to enhance Kv1.2 currents in the presence of the T46V mutation may have resulted from the change in biophysical properties rather than elimination of a phosphorylation site *per se*. Alternatively, Connors *et al.* (27) reported that the T46V mutation blocked forskolin-induced increase in surface expression of Kv1.2 by interfering with trafficking (27). Here, we have employed a biochemical approach to directly analyze phosphorylation of the wild-type channel using a combination of phosphopeptide mapping, phosphoamino acid analysis, analysis of *in vitro* ^{32}P incorporation into WT and mutant proteins, and direct sequencing by mass spectrometry of *in vitro*- and *in situ*-phosphorylated proteins. Phosphoamino acid analysis of wild-type Kv1.2 after *in vitro* PKA-catalyzed phosphorylation did not detect threonine phosphorylation, and the T46V mutation did not affect ^{32}P incorporation. We were also unable to detect *in situ* phosphorylation at Thr-46 in wild-type Kv1.2 in the absence or presence of PKA activation using LC-MS/MS or MIDAS analysis. This result is consistent with previous proteomic analysis of brain and recombinant Kv1.2 that also failed to detect Thr-46 phosphorylation (26, 27).

In summary, our combined biochemical and patch clamp analyses indicate a role for Ser-449 in the C terminus of Kv1.2 as a site for modulation of channel activity by PKA-catalyzed phosphorylation. The increase in current amplitude due to phosphorylation of the channel subunit is distinct from previously reported mechanisms that alter surface expression of Kv1.2 (26, 27). A role for the C terminus in modulation of channel gating has been demonstrated for other Kv channels, including Kv2.1 (37, 38), and this may depend on an interaction of the C terminus with the S4-S5 segment of adjacent subunits (39). It is possible that phosphorylation of Ser-449 in the C terminus of Kv1.2 alters this interaction to increase channel activity. Further studies will be required to determine whether this is the mechanism involved.

REFERENCES

1. Nelson, M. T., and Quayle, J. M. (1995) *Am. J. Physiol.* **268,** C799–C822
2. Knot, H. J., and Nelson, M. T. (1995) *Am. J. Physiol.* **269,** H348–H355
3. Davis, M. J., and Hill, M. A. (1999) *Physiol. Rev.* **79,** 387–423
4. Kerr, P. M., Clément-Chomienne, O., Thorneloe, K. S., Chen, T. T., Ishii, K., Sontag, D. P., Walsh, M. P., and Cole, W. C. (2001) *Circ. Res.* **89,** 1038–1044
5. Thorneloe, K. S., Chen, T. T., Kerr, P. M., Grier, E. F., Horowitz, B., Cole, W. C., and Walsh, M. P. (2001) *Circ. Res.* **89,** 1030–1037
6. Albarwani, S., Nemetz, L. T., Madden, J. A., Tobin, A. A., England, S. K., Pratt, P. F., and Rusch, N. J. (2003) *J. Physiol.* **551,** 751–763
7. Plane, F., Johnson, R., Kerr, P., Wiehler, W., Thorneloe, K., Ishii, K., Chen, T., and Cole, W. (2005) *Circ. Res.* **96,** 216–224
8. Hayabuchi, Y., Standen, N. B., and Davies, N. W. (2001) *Am. J. Physiol. Heart Circ. Physiol.* **281,** H2480–H2489
9. Luykenaar, K. D., Brett, S. E., Wu, B. N., Wiehler, W. B., and Welsh, D. G. (2004) *Am. J. Physiol. Heart Circ. Physiol.* **286,** H1088–H1100
10. Aiello, E. A., Walsh, M. P., and Cole, W. C. (1995) *Am. J. Physiol.* **268,** H926–H934
11. Aiello, E. A., Clément-Chomienne, O., Sontag, D. P., Walsh, M. P., and Cole, W. C. (1996) *Am. J. Physiol.* **271,** H109–H119
12. Aiello, E. A., Malcolm, A. T., Walsh, M. P., and Cole, W. C. (1998) *Am. J.*

Physiol. **275,** H448–H459

13. Cole, W. C., Clément-Chomienne, O., and Aiello, E. A. (1996) *Biochem. Cell Biol.* **74,** 439–447

14. Dong, H., Waldron, G. J., Cole, W. C., and Triggle, C. R. (1998) *Br. J. Pharmacol.* **123,** 821–832

15. Satake, N., Shibata, M., and Shibata, S. (1996) *Br. J. Pharmacol.* **119,** 505–510

16. Li, H., Chai, Q., Gutterman, D. D., and Liu, Y. (2003) *Am. J. Physiol. Heart Circ. Physiol.* **285,** H1213–1219

17. Heaps, C. L., and Bowles, D. K. (2002) *J. Appl. Physiol.* **92,** 550–558

18. Heaps, C. L., Tharp, D. L., and Bowles, D. K. (2005) *Am. J. Physiol. Heart Circ. Physiol.* **288,** H568–576

19. Berg, T. (2003) *Eur. J. Pharmacol.* **466,** 301–310

20. Du, C., Carl, A., Smith, T. K., Sanders, K. M., and Keef, K. D. (1994) *J. Pharmacol. Exp. Ther.* **268,** 208–215

21. Koh, S. D., Sanders, K. M., and Carl, A. (1996) *Pflugers Arch.* **432,** 401–412

22. Shuttleworth, C. W., Koh, S. D., Bayginov, O., and Sanders, K. M. (1996) *J. Physiol.* **493,** 651–663

23. Huang, X. Y., Morielli, A. D., and Peralta, E. G. (1994) *Proc. Natl. Acad. Sci. U. S. A.* **91,** 624–628

24. Kennelly, P. J., and Krebs, E. G. (1991) *J. Biol. Chem.* **266,** 15555–15558

25. Minor, D. L., Lin, Y. F., Mobley, B. C., Avelar, A., Jan, Y. N., Jan, L. Y., and Berger, J. M. (2000) *Cell* **102,** 657–670

26. Yang, J. W., Vacher, H., Park, K. S., Clark, E., and Trimmer, J. S. (2007) *Proc. Natl. Acad. Sci. U. S. A.* **104,** 20055–20060

27. Connors, E. C., Ballif, B. A., and Morielli, A. D. (2008) *J. Biol. Chem.* **283,** 3445–3453

28. Chen, T. T., Luykenaar, K. D., Walsh, E. J., Walsh, M. P., and Cole, W. C. (2006) *Circ. Res.* **99,** 53–60

29. Xiao, B., Jiang, M. T., Zhao, M., Yang, D., Sutherland, C., Lai, F. A., Walsh, M. P., Warltier, D. C., Cheng, H., and Chen, S. R. (2005) *Circ. Res.* **96,** 847–855

30. Colburn, J. C., Michnoff, C. H., Hsu, L. C., Slaughter, C. A., Kamm, K. E., and Stull, J. T. (1988) *J. Biol. Chem.* **263,** 19166–19173

31. Boyle, W. J., van der Geer, P., and Hunter, T. (1991) *Methods Enzymol.* **201,** 110–149

32. Erickson, A. C., and Johnson, G. V. (1993) *J. Neurosci. Methods* **46,** 245–249

33. Allen, B. G., Andrea, J. E., and Walsh, M. P. (1994) *J. Biol. Chem.* **269,** 29288–29298

34. Demaille, J. G., Peters, K. A., Strandjord, T. P., and Fischer, E. H. (1978) *FEBS Lett.* **86,** 113–116

35. Unwin, R. D., Griffiths, J. R., Leverentz, M. K., Grallert, A., Hagan, I. M., and Whetton, A. D. (2005) *Mol. Cell. Proteomics* **4,** 1134–1144

36. Anderson, A. E., Adams, J. P., Qian, Y., Cook, R. G., Pfaffinger, P. J., and Sweatt, J. D. (2000) *J. Biol. Chem.* **275,** 5337–5346

37. Ju, M., Stevens, L., Leadbitter, E., and Wray, D. (2003) *J. Biol. Chem.* **278,** 12769–12778

38. VanDongen, A. M., Frech, G. C., Drewe, J. A., Joho, R. H., and Brown, A. M. (1990) *Neuron* **5,** 433–443

39. Zhao, L. L., Wu, A., Bi, L. J., Liu, P., Zhang, X. E., Jiang, T., Jin, G., and Qi, Z. (2009) *Mol. Memb. Biol.* **26,** 186–193

Identification and Functional Characterization of Protein Kinase A-catalyzed Phosphorylation of Potassium Channel Kv1.2 at Serine 449

Rosalyn P. Johnson, Ahmed F. El-Yazbi, Morgan F. Hughes, David C. Schriemer,
Emma J. Walsh, Michael P. Walsh and William C. Cole

Access the most updated version of this article at doi: 10.1074/jbc.M109.010918

Alerts:
- When this article is cited
- When a correction for this article is posted

Click here to choose from all of JBC's e-mail alerts

This article cites 39 references, 21 of which can be accessed free at
http://www.jbc.org/content/284/24/16562.full.html#ref-list-1